Journal Pre-proof

In-situ gelling xyloglucan formulations as 3D artificial niche for adipose stem cell spheroids

F. Toia, A.B. Di Stefano, E. Muscolino, M.A. Sabatino, D. Giacomazza, F. Moschella, A. Cordova, C. Dispenza

PII: S0141-8130(20)34806-6

DOI: https://doi.org/10.1016/j.ijbiomac.2020.10.158

Reference: BIOMAC 17048

To appear in: *International Journal of Biological Macromolecules*

Received date: 25 June 2020

Revised date: 16 October 2020

Accepted date: 20 October 2020

Please cite this article as: F. Toia, A.B. Di Stefano, E. Muscolino, et al., In-situ gelling xyloglucan formulations as 3D artificial niche for adipose stem cell spheroids, *International Journal of Biological Macromolecules* (2018), https://doi.org/10.1016/j.ijbiomac.2020.10.158

In-situ gelling xyloglucan formulations as 3D artificial niche for adipose stem cell spheroids

F. Toia [1,2#] A.B. Di Stefano[2#], E. Muscolino[3], M.A. Sabatino[3], D. Giacomazza[4], F. Moschella[2], A. Cordova[1,2], C. Dispenza [3 4, *]

[1]Dipartimento di Discipline Chirurgiche, Oncologiche e Stomatologiche, Università degli Studi di Palermo, Università degli Studi di Palermo, via del Vespro 129, 90127, Palermo, Italy.

[2]BIOPLAST-Laboratory of BIOlogy and Regenerative Medicine-PLASTic Surgery, Dipartimento di Discipline Chirurgiche, Oncologiche e Stomatologiche, Università degli Studi di Palermo, Università degli Studi di Palermo, via del Vespro 129, 90127, Palermo, Italy.

[3]Dipartimento di Ingegneria, Università degli Studi di Palermo, Viale delle Scienze 6, 90128 Palermo, Italy.

[4]Istituto di BioFisica, Consiglio Nazionale delle Ricerche, Via U. La Malfa 153, 90146 Palermo, Italy.

[#] These authors contributed equally to this work.

* Corresponding author: clelia.dispenza@unipa.it

Abstract

Three-dimensional spheroidal cell aggregates of adipose stem cells (SASCs) are a distinct upstream population of stem cells present in adipose tissue, with enhanced regeneration properties *in vivo.* The preservation of the 3D structure of the cells, from extraction to administration, can be a promising strategy to ensure optimal conditions for cell viability and maintenance of stemness potential. With this aim, an artificial niche was created by incorporating the spheroids into an injectable, in-situ gelling solution of partially degalactosylated xyloglucan (dXG) and an *ad hoc* formulated culture medium for the preservation of stem cell spheroid features. The evolution of the mechanical properties and the morphological structure of this artificial niche was investigated by small amplitude rheological analysis and scanning electron microscopy, respectively. Comparatively, systems produced with the same polymer and the typical culture medium (DMEM) used for adipose stem cell growth in adherent cell culture conditions (ASC) were also characterised. Cell viability of both SASCs and ASCs incorporated inside the hydrogel or seeded on top of the hydrogel were investigated as well as the preservation of SASC stemness conditions when embedded in the hydrogel.

Keywords

Spheroids of adipose stem cells, artificial niche, in-situ forming gel, partially degalactosylated xyloglucan.

Introduction

Tissue-engineering aims at identifying the best combination of cells and scaffolds to allow cell growth and ultimately creation of new tissue. Mesenchymal stem cells (MSCs) are increasingly used as cellular components in tissue engineering owing to their multilineage differentiation and regenerative potential [1]. Adipose tissue-derived MSCs (ASCs) are particularly attractive for their high concentration in the tissue and ease of harvesting, resulting in timely availability and cost-effectiveness [2]. In general, ASCs are first isolated, then seeded and cultured as two-dimensional (2D) adherent monolayers on flat and rigid substrates and finally either directly administered or implanted/injected in combination with

a scaffold [3, 4]. When ASCs are cultivated in low adhesion flasks with a suitable culture medium they aggregate in the form of spheroids (SASCs). These culture conditions, that provide stem cells with a constant 3D environment from harvesting to administration, seem to be beneficial for stem cells to be used in regenerative medicine. In fact, SASCs have demonstrated an increased early differentiation potential towards all mesenchymal lineages and enhanced bone regeneration properties *in vivo* in comparison to adherent ASCs or SASC–derived osteoblasts [5, 6]. They represent a distinct upstream population of ASCs, exhibiting the microRNA and mRNA profiles of highly undifferentiated cells, which explains their potency [7].

Direct administration of stem cells presents several limitations and potential risks, including short cell survival rates, low residence time after administration, uncontrolled cell spreading, poor interaction and integration with the surrounding tissue, and differentiation into undesirable tissue [8-11]. The use a porous biomaterial as a scaffold limits cell dispersion upon administration and serves as a mechanical structural support [12]. It also provides cells with tissue-specific mass transport properties, through its interconnected porosity, granting oxygen and nutrient supply and waste removal. It protects the cells from the eventual hostile local microenvironment and from the attack of the host immune system. Moreover, the additional dimensionality of the scaffold, its stiffness and the eventual presence of specific signaling molecules can improve MSCs differentiative and regenerative abilities [13, 14].

Hydrogels can meticulously look like the native ECM, due to their hydration, interconnected pore architecture and biocompatibility [15]. For this reason, they have been explored extensively as ECM mimics, to investigate the mechanical and biochemical aspects of the cellular environment on cell function, both *in vitro* and *in vivo*, and for the development of new tissue [16-18]. Hydrogels used as artificial ECM of MSCs, also called *niche,* can be either decellularized ECMs (dECM), derived from allogenic or xenogenic tissues, e.g. skin, cartilage, small intestinal submucosa or amniotic membrane [19-21], or can be fabricated from synthetic- and/or natural-origin polymers [22-24]. If injectable, in situ forming hydrogels are employed, stem cell retention and optimal microenvironment reconstruction can be achieved with minimal invasiveness and with the convenience to reach uneven, and/or difficult to access lesions [25, 26]. An interesting approach is based on the synthesis of hybrid systems based on β-cyclodextrine host-guest interactions to attach various inductive peptides onto thermo-responsive poly(organophosphazene)s. Yet, the advantage of high flexibility in designing the artificial niche is counteracted by the recourse to a complex chemistry [27]. Engineering injectable artificial *niches* using biocompatible, vegetal-source polymers that can form physical gels under physiological conditions, without addition of crosslinkers, sugar or alcohols, is a particularly attractive strategy. It limits the risks of an immunogenic response and it reduces the number of components and process operations to a minimum, making the management of scale-up and regulatory aspects easier.

Xyloglucan (XG) is a very common polysaccharide present in the cell walls of superior plants as crosslinker of adjacent cellulose microfibrils and in seeds as storage compound. Xyloglucan from tamarind seeds (TS-XG) is commercially available, non-toxic, biodegradable [28, 29] and FDA-approved as food additive [30]. TS-XG is composed of a α β-(1, 4)-D-glucan backbone that is partially substituted by α-(1, 6)-D-xylose. In addition, some of the xylose

residues are substituted by β-(1, 2)-D-galactoxylose [28, 31]. The hydrophilic galactosylated side branches provide the polymer with "water-solubility" (see inset in Figure 1). When a fraction of the galactose residues are removed by fungal β-galactosidase [32, 33], the partially degalactosylated xyloglucan (dXG) forms thermo-reversible gels. In particular, for a galactose removal ratio (GRR) between 35% and 50%, and polymer concentrations of 1 %w and higher, the macroscopic gelation occurs at body temperature [33]. Owing to the favorable gelling behavior and biocompatibility, dXG hydrogels have been already evaluated as *in-situ* forming drug delivery depots [29, 34-38] or scaffolds for the reconstruction of soft tissues [39-41]. It is also worth mentioning that dXG has also shown interesting inherent immunomodulatory activity [42].

In this work, SASCs were mixed with an aqueous dXG dispersion and an equal volume of an in house-developed "stem cell medium" (SCM) containing biochemical factors to preserve the stem cell spheroid morphology and stemness features [43]. In order to assess the potential benefits originating from SASCs as the cellular component analogous systems were prepared using the more conventional ASCs, and DMEM as culture medium. To assess the homing ability of dXG hydrogels in case of sequential but separate injections of hydrogel precursors and cells, SASC and ASC cells were seeded on the surface of the pre-formed dXG hydrogels and cultivated with SCM and DMEM, respectively (see Figure 1). Prior to the evaluation of stem cell viability, mechanical and morphological characterisations of dXG hydrogels were performed by small amplitude rheological analysis and scanning electron microscopy, respectively. The influence of culture media on the hydrogel structure and its evolution with time at 37°C was investigated in consideration of the important role that the biomechanical and biochemical properties of the micro-environment play on stem cells viability. The ability of the in-situ forming scaffold to preserve the stemness features when SASCs are embedded in the hydrogel was also investigated by gene and protein expression analysis of pluripotency related markers. Finally, the injectability of dXG dispersions loaded with SACSs was evaluated by measuring the shear viscosity of the mixture, assessing the rheological properties of the hydrogels formed in the presence of the SASCs from the injected dispersions and cell viability over a time span of 21 days from the time of injection.

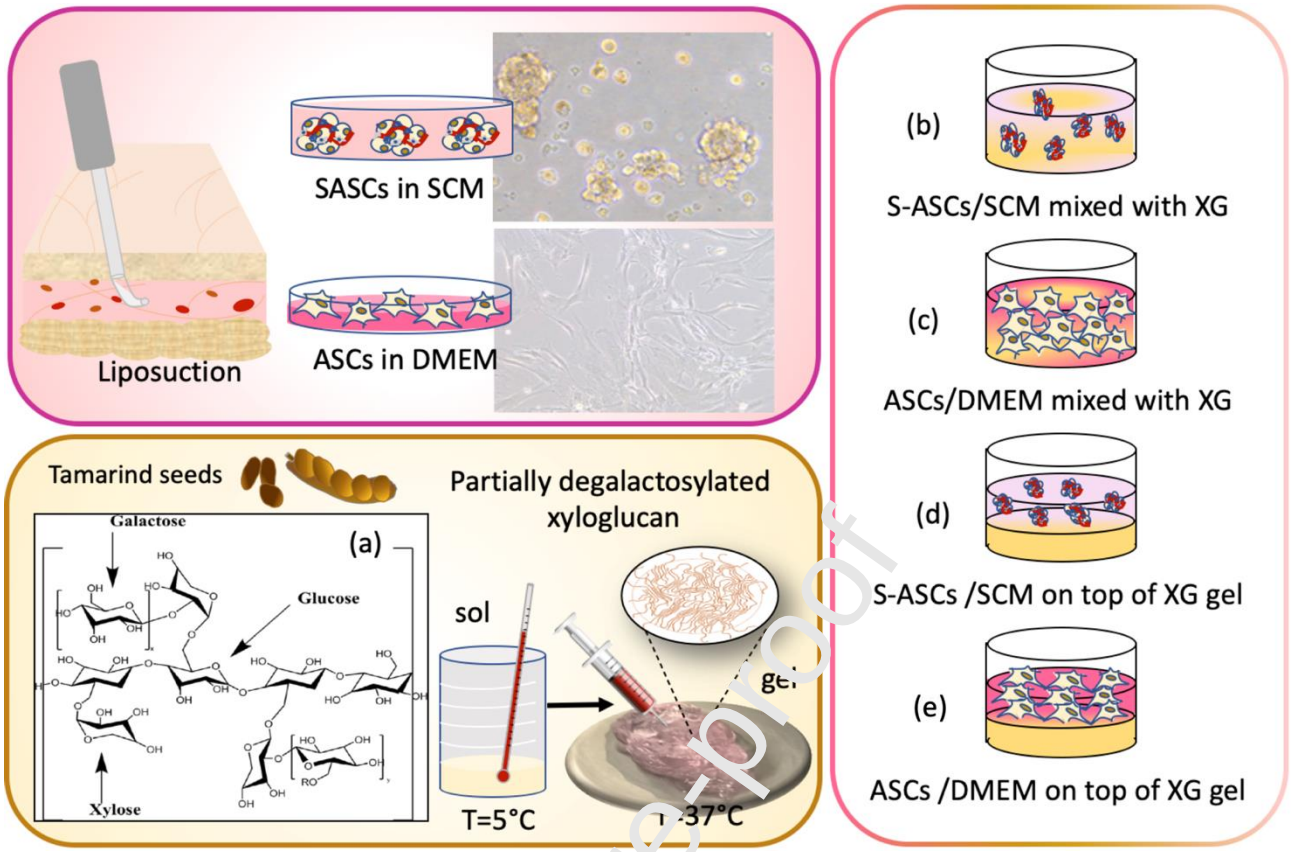

Figure 1. Schematic representation of the integration of injectable, in-situ forming partially degalactosylated tamarind seed xyloglucan (dXG) gels with spheroids of human adipose stem cells (SASCs) or adherent human adipose stem cells (ASCs). "Mixed systems" (b, c) are obtained by incorporation of cells in the sol phase at 20°C, while "up systems" (d and e) are obtained by seeding cells on the already formed gel at 37°C. SASCs were always compounded with SCM (b, d), and ASCs with DMEM (c, e). In the inset (a), the chemical structure of the glycosylated unit of TS-XG.

2. Materials and methods

2.1. Materials

Tamarind seeds xyloglucan was purchased from Megazyme International (Ireland). Sugar composition of the tamarind seed xyloglucan is xylose 34 %w; glucose 45 %w; galactose 17 %w; arabinose and other sugars 4 %w, as provided by Megazyme International. β-Galactosidase from Aspergillus oryzae (11.8 U/mg) was purchased from Sigma Chemicals (USA). Tamarind seeds xyloglucan was degalactosylated according to an established protocol, to obtain a degalactosylated degree of ca. 45% [33, 44].

2.2 Cell cultures

Adipose tissue was collected from healthy individuals, following approval of an informed consensus. Lipoaspirate samples were harvested from different body areas such as abdomen, breast, flanks, trochanteric region. After mechanic (shake 30 minutes at 37°C) and enzymatic (collagenase 150 mg/ml, Gibco, Carlsbad, CA) digestion, the samples were centrifuged at 1200 rpm for 5 minutes and the stromal vascular fraction (SVF) was resuspended in specific medium. For 3D cultures, the SASCs were plated in stem cell medium (SCM) composed

principally by DMEM/F12 salts with added basic fibroblast growth factor (bFGF, 10 ng/ml; Sigma, St. Louis, MO) and epidermal growth factor (EGF, 20 ng/ml, Sigma) [43]. SASCs were grown as fluctuating spheroids in an ultra-low attachment culture flask (Corning, NY) [5]. While for 2D cultures, the SVF was plated in DMEM and FBS (10%) in adherent cell culture conditions. All systems were added of a small volume of Antibiotic-Antimycotic solution (1X, Gibco) to prevent bacterial and fungal contamination. Culture flasks were placed at 37°C in a humidified 5% CO_2 incubator.

2.3 Hydrogel preparation

dXG powder was dissolved in 0.22 μm pre-filtered water at 2 %w concentration, by magnetic stirring for about 2 hours in an ice bath, then autoclaved at 120°C for 20 minutes to attain homogenous dispersion and sterility. dXG systems cannot be strictly considered solutions, i.e. completely devoid of chain aggregates. This is due to the presence of galactose-bare sequences in the chains that cause side-by-side association of few segments of different chains forming condensed domains [45, 46]. The dispersions were stored at 4°C.

Known volumes of the 2 %w polymeric dispersion were either incubated at 37°C for 10 min (dXG2 T0) or gently mixed with the same volume of water, SCM, or DMEM and then incubated at 37°C for 10 min before any further use. After 10 min, for both systems, macroscopic gelation has occurred [41]. The "mixed systems" were analysed immediately (T0) and after incubation at 37°C for 7 days (T7) and 21 days (T21). Each system is named after as dXG1-Z, where 1 indicates the final polymer concentration in weight percentage and Z is a letter referring to the swelling/culture medium that has been mixed with the 2 %w dXG dispersion. In particular, W stands for water, S for SCM and D for DMEM.

Known volumes of the dXG2 T0 hydrogels were covered with the same volume of each of the aforementioned media (water, SCM or DMEM) and incubated at 37°C for 7 days (T7) and 21 days (T21). These systems are identified as dXG2UP-Z, where 2 refers to the weight percent of the polymer in the original aqueous polymeric dispersions, UP indicates that the medium that is added on top of the dXG2 T0 hydrogel, and Z refers to the various swelling/culture media. Table 1 shows the composition of all investigated systems in terms of polymer concentration, volume percentage of the added medium, content of proteins, glucose and main inorganic salts.

Table 1. Final composition of the hydrogels

Code	Deg-XG, %w	Water, % w	Medium, %v	Salts (g/l)	Glucose (g/l)	Aminoacids (g/l)
dXG1-W	1	99	\	\	\	\
dXG1-S	1	49	50	3.466	2.465	0.837
dXG1-D	1	49	50	10.100	4.500	5.570
dXG2	2	98	\	\	\	\

2.4 Rheological analysis

The rheological analysis in small-oscillatory conditions was carried out using a stress-controlled Rheometer AR G2 (TA Instruments). The geometry used was a steel plate of 20 mm diameter with a gap of ~500 μm. As a preliminary step in the analysis, strain sweep measurements were carried out to identify measurement conditions where there is

independence of instrumental responses of oscillation amplitude, i.e. the limit of linear viscoelastic regime (LVR). These measurements were executed at 37.0±0.1°C and 1 Hz. The strain was swept between 0.001 and 0.01. Frequency sweeps were then performed at $7x10^{-3}$ strain (within LVR for all systems) between 0.1 Hz and 10 Hz. Known volumes of the dispersions were poured on the instrument and measurements started after 10 minutes of thermal and structural equilibration at 37°C.

2.5 Morphological analysis

Hydrogels microstructure was investigated using a Field Emission Scanning Electron Microscope (SEM) Phenom ProX desktop at an accelerating voltage of 10kV. The hydrogels were frozen in liquid nitrogen, freeze-dried, mounted on aluminium stubs and gold coated by JFC-1300 gold coater (JEOL) for 120 s at 30 mA before scanning.

2.6 Stem cells loading, incubation and recovery

Cells were loaded either by mixing dXG2 with the same volume of SASC-3D or ASC-2D suspension in SCM and DMEM (named after as SASCs-3D dXG1-S and ASCs-2D dXG1-D), respectively; or by forming a dXG2 hydrogel slab directly on the cell culture well and adding on top the SASC-3D or ASC-2D suspension (named after SASCs-3D dXG2UP-S and ASCs-2D dXG2UP-D). In both cases ca. 50000 cells/well were loaded and maintained in CO_2 incubator at 37°C for 1 day, 7 days and 21 days. Cell proliferation was monitored under a light microscope (Leica DM IL LED Fluo).

The recovery of cells from "mixed systems" was performed by incubation with an aqueous solution of Cellulase from Trichoderma reesei (Sigma Aldrich) at a final concentration of 84 U/ml for 90 minutes at 37°C, centrifugation at 1200 RPM for 5 minutes at 4°C and removal of the surnatant dispersion. In order to evaluate eventual effects of the enzymatic treatment on cells, the same protocol has been applied to SASCs and ASCs and their viability was confirmed by cell count with trypan blue.

2.7 Cell viability evaluation

Cell viability of SASCs and ASCs was quantified with MTS test (3-(4,5-dimethylthiazol-2-yl)-5-(3-carboxymethoxyphenyl)-2-(4-sulfophenyl)-2H-tetrazolium)(Biorad). Cells were plated in biological triplicates at a density of 50000 cells/well in 96-well plates filled either with 100 µl/well of culture medium (control) or 50 µl/well of hydrogel and 50 µl/well of culture medium. The absorbance at 490nm was analysed at 1 day, 7 days and 21 days of incubation.

Cells recovered from "mixed systems" incubated for 21 days were resuspended in 1X Binding Buffer and stained with 5µl of APC-Annexin V (BioLegend) and 10µl of Propidium Iodide (PI) (BioLegend) for 15 minutes at room temperature in the dark, to evaluate the apoptotic and necrotic cells. The cells were counterstained with Hoechst dye (10 minutes), covered with a glass coverslip and visualized with Nikon A1 confocal microscope.

2.8 mRNA expression profile

Total RNA was extracted from SASCs recovered from the hydrogel using RNeasy Mini Kit (Qiagen) and quantified using fluorometer Qubit4 (Invitrogen). 175 ng of RNA was retrotranscribed in cDNA through the High Capacity cDNA Reverse Transcription kit (Applied

Biosystems). The qPCR reactions were all performed in triplicate. The predesigned Taqman primers (Thermo Fisher) were: SOX2 Hs01053049_s1; POU5F1 Hs00999632_g1; NANOG Hs04399610_g1 as stemness markers and GAPDH Hs02758991_g1 as housekeeping gene. The relative expression levels of mRNAs were calculated using the $2^{-\Delta\Delta Ct}$ Livak method [47].

2.9 Immunofluorescence staining

In order to characterize the SASCs stemness in "mixed" conditions, cell-laden hydrogels were plated in chambered cover-glasses (Lab-Tek II Chambered Coverglass) which allow to analyse living cells with ideal optical characteristics required for confocal image analysis. After 21 days of culture in SCM medium, the samples were fixed in formalin for 10 minutes at room temperature (RT). Then, they were permeabilized with Triton-X100 0.1% and exposed to rabbit anti-human SOX2 antibody (SantaCruz) overnight at 4°C. After incubation to Goat Anti-Rabbit, Alexa fluor Plus 568 (Thermofisher Scientific) secondary antibody for 2h at RT, the nuclei were counterstained with Hoechst for 10 minutes at RT. The immunofluorescence analysis was conducted with confocal microscope.

2.10 Statistical analysis

Data are expressed as mean ± standard deviation of three independent experiments. Statistical significance was calculated using one-way analysis of variance (ANOVA), followed by either a Tukey's or Bonferroni's multiple comparison post hoc test. Significance levels were analysed with GraphPad Prism 5 statistical software and indicated as p values (*$p < 0.05$, **$p < 0.01$, and ***$p < 0.001$).

2.11 Injectability

The injectability of dXG1-S was evaluated by measuring the shear viscosity of the dispersion without and with SASCs (ca. 500000 cells/ml), the storage and loss moduli from rheological analysis of cell-laden and cell-devoid hydrogels formed after injection, and cell viability by MTS analysis of injected SASCs-3D dXG1-S. The injection was carried out with 2.5 ml polypropylene syringes equipped with G23 needles loaded with gently pre-mixed SASCs-3D dXG1-S dispersions. Shear viscosity measurements were performed using the stress-controlled Rheometer AR G2 in rotational mode at constant temperature of 25.0±0.1°C. Samples of dXG1-S dispersion, with and without SASCs, were placed on a 20 mm diameter plate with a gap of ~500 μm. Rheological analysis in small-oscillatory conditions was carried out as described in section 2.4. Samples were directly injected at ca. 25°C on the rheometer plate and let equilibrate at 37.0±0.1°C for 10 minutes. Cell viability of the SASCs-3D dXG1-S dispersions injected in 96-well plates was assessed by MTS test as described in section 2.7.

Results and discussion

3.1 Mechanical and morphological characterisation of the as prepared hydrogels

Rheological measurements in small-amplitude oscillatory shear conditions were carried out on hydrogel samples formed directly on the rheometer plate set a 37°C from aqueous dispersions of partially degalactosylated xyloglucan. In Figure 2a the storage modulus, G', and loss modulus, G", curves as function of frequency for dXG1-W and dXG2 systems are reported. dXG2 shows frequency-invariant G' and G" curves, with G' approximatively one order of

magnitude higher than G". This rheological behaviour is associated to the formation of a stable network (with long living crosslinking points). dXG1-W has lower G' and G" values than dXG2, with G" approaching G' at higher frequencies. In the frequency range probed, dXG1-W is responding as weak and more heterogeneous network, with crosslinks characterised by a wide range of lifetimes [48].

Figure 2b-c displays the morphology of the dXG1-W T0 and dXG2 T0 cross-sections. dXG1-W shows an ordinary, random 3D network of interconnected pores with thin walls. The system can be considered isotropic and, from a close look, shows shreds of thin membranes. dXG2 presents a more compact structure with a multi-layered morphology. The layers are formed by thin membranes with inhomogeneous porosity and only spare interconnections. The spatial separation among the layers is also fairly inhomogeneous. The development of a membrane-structured morphology seems to be related to polymer concentration. Concentrated dXG colloidal dispersions can be described as mainly composed of ribbon-like aggregates of ellipsoid-like condensed domains with a tendency to bind and stack in parallel [49, 50]. The increase of temperature modifies the balance between hydrophilic and hydrophobic interactions inducing contraction and further association of flat ribbon-like aggregates to form membranes and polymer-depleted interphase regions. It appears that extended membranes can only form if the local polymer concentration is sufficiently high and gelation not too fast to impede chain disentanglements and reorganisation.

The more compact structure of dXG2 compared to dXG1-W and the orientation of some layers perpendicular to the shear plane impose distortion of the layer stacks and explain the higher values of G' and G".

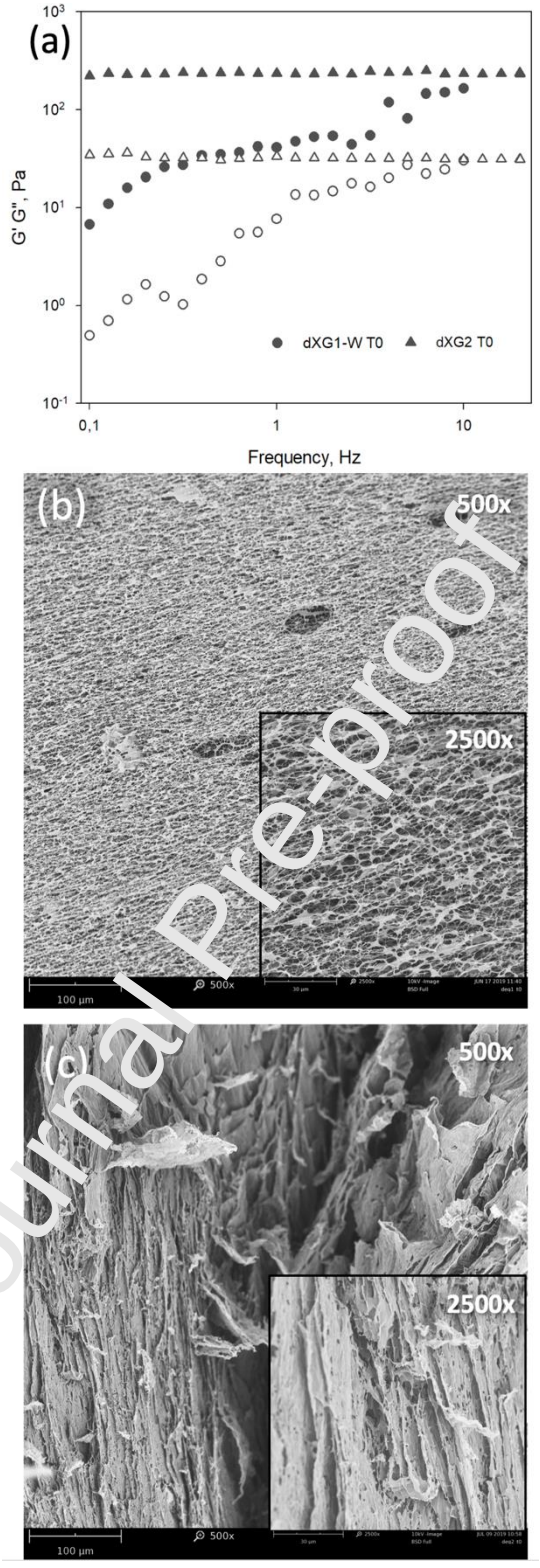

Figure 2. (a) Storage modulus, G' (full dot), and loss modulus, G" (hollow dot), of dXG1-W T0 and dXG2 T0 as function of frequency; (b) Morphology of T0 dXG1-W at x500 and x2500 magnification; (c) Morphology of T0 dXG2 at x500 and x2500 magnification.

3.2 Influence of the culture media on network formation

In order to provide SASCs and ASCs with a microenvironment that can guarantee their survival, dXG gels were loaded with the components present in their typical culture media, i.e.

salts, glucose and various aminoacids. In particular, adherent ASCs are generally cultured in DMEM, while for SASCs an *in house* developed medium was considered [43].The final hydrogel formulations are the result of either mixing the 2%w dXG aqueous dispersion with an equal volume of either SCM or DMEM ("mixed-systems") or of the addition of the same volume of the culture medium on top of the already gelled system ("up-systems"). ~~The "mixed systems" provide, already from the beginning of the experiment, the maximum contact area between hydrogel and cells, whereas for the "up-systems" this contact area is much reduced (and cell-to-cell contact is increased).~~ Since we expect that the various components present in the culture media can influence the initial network organisation and its development over time, the rheological and morphological properties of dXG gels formed in the presence of ("mixed-systems") or exposed to ("up-systems") the two culture media were investigated and compared with systems containing only the polymer and water. The "up-systems" were allowed to equilibrate for 7 days before analysis and were characterised again after 21 days, as it will be described in the following section. The "mixed systems" were characterised at T0, i.e. ten minutes after compounding, after 7 days (T7) and 21 days (T21) of incubation at 37°C.

Figure 3a shows the rheological behaviour in small amplitude oscillation conditions for dXG1-S T0 and dXG1-D T0. The curves relative to dXG1-W T0 are also reported, for comparison. The rheological behaviour of all systems is characteristic of weak gels: G' curves are higher than G" curves and show frequency-dependence", generally associated to networks with a wide range of relaxation times. dXG1-D shows the highest values of both storage and loss moduli. No significant differences between the G' curves of dXG1-S and dXG1-W can be evidenced, while G" curve for dXG1-S is more frequency-dependent. It can be argued that the components of DMEM, and their higher concentration with respect to SCM, affect the polymeric network structure leading to a stronger hydrogel. The identification of the specific cause of the observed effects is arduous, being most likely the result of a combination of several factors. In facts, amino acids, sugars and salts can have a profound influence on the gelation of polysaccharides, due to purely entropic effects (salting out effects or ion-mediated depletion forces) and/or by disrupting polymer-solvent H-bonding interactions. The induced polymer chain conformational changes can be the cause of further intra-/inter-molecular aggregation [51-53].

The morphological analysis of the systems confirms the strong effect of the media on network organisation. SEM micrographs of sample cross-sections are shown in Figure 4. dXG1-D T0 shows a strong fibrillar network. The formation of fibrillar structures, induced by the combined presence of kosmotropic salts and an increase of temperature up to ca. 50°C, was also observed for the native XG by Sakakibara et al. [54]. XG was described to display a conformational transition from a helical structure to a chain extended conformation upon heating, that was sensitive to the presence of the anions of the salt present in the medium [54]. dXG1-S T0 shows a morphology that can be described as the result of the structural collapse of extended hollow membranes formed by fusion of flat ribbons and fibrils, a collapse that is likely caused by the freeze-drying process. The size of the holes and the thickness of the membranes appear to be very heterogeneous. The existence of heterogenous micro-domains, with local density variations, can explain the observed marked frequency-dependence of both G' and G".

3.3 Influence of incubation time on hydrogel structure

Figure 3b-d shows the mechanical spectra of dXG1-W, dXG1-S and dXG1-D after 7 days and 21 days of incubation at 37°C, that are the same incubation times chosen for cell viability tests. The curves relative to the corresponding T0 systems are also reported for comparison. Changes over time in the viscoelastic behaviour of these systems are to be expected, considering that the gelation process is fairly rapid and "freeze" the systems in a structure that can be very far from equilibrium. During the prolonged incubation at 37°C cooperative chain segment dynamics can be activated, and the network structure modified both in terms of strength and density of crosslinking points. We expect the network rearrangements to have an impact on hydrogel stiffness and morphology. The swelling medium equilibrates also with the gaseous atmosphere in the incubation chamber and this may introduce further perturbations, like the formation of a drier skin layer. Moreover, the polymer chains at the gas atmosphere-hydrogel interface may rearrange as a consequence of its hydrophobicity.

For dXG1-W (Figure 3b), G' and G" curves are higher after 7-day incubation, suggesting that the polymer chains have undergone organised rearrangements with the formation of a stronger network. After two further weeks of incubation, both G' and G" plots have decreased, probably due to further molecular rearrangements.

A different behaviour is observed for dXG1-D (Figure 3c) and dXG1-S (Figure 3d). For dXG1-D, both storage and loss modulus plots progressively decrease with time**.** For dXG1-S (Figure 3d) they progressively increase, and after 21-day incubation the two curves become frequency-independent, with one order of magnitude difference between the two. While differences between the three systems are not very significant after 7 days of incubation (Figure 3e), they become more important after 21 days of incubation, with dXG1-S T21 resulting in the stiffest hydrogel of the three (Figure 3f).

The morphology evolution of the systems can provide hints to interpret the observed differences in the mechanical spectra (see Figure 4). SEM micrographs of dXG1-W cross-sections after 7 days incubation show portions of the sample that still resemble the T0 system (see inset of dXG1-W T7 in Figure 4) and other portions are characterised by a highly ordered morphology, with stacked layers interconnected by uniformly distributed orthogonal walls. After 21 days, the structure is characterised by random and wide porosity and large shreds of thin membranes. The presence of more compact domains can explain the increase in storage modulus for dXG1-W T7, while the heterogeneity in the morphology is in good agreement with the strong frequency-dependence of G". On the contrary, the more widely open porosity of the dXG1-W T21 explains the observed reduction in both storage and loss moduli. Significant changes in the morphology are also seen for dXG1-D and dXG1-S. The former system evolves towards a more open 3D porous structure, that explains the progressively lower values of storage and loss moduli. The dXG1-S system shows the formation of large, phase-separated domains, that eventually collapse with an increase in local polymer concentration and network stiffness.

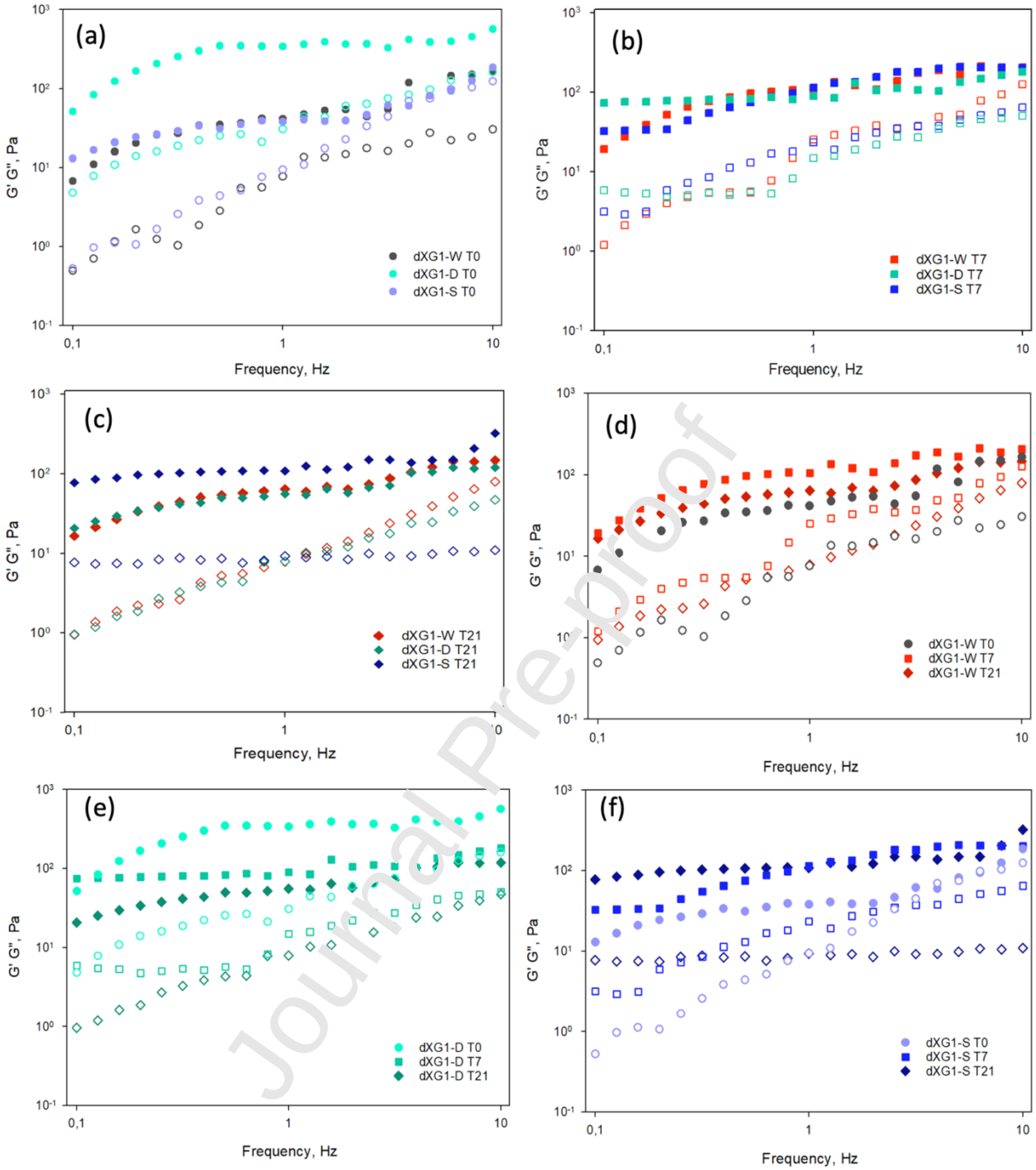

Figure 3. Storage modulus, G' (full dot), and loss modulus, G" (hollow dot), as a function of frequency for "mixed systems" produced with the three swelling media and three incubation times: (a) dXG1-W T0, dXG1-D T0 and dXG1-S T0; (b) dXG1-W T0, T7 and T21; (c) dXG1-D T0, T7 and T21; (d) dXG1-S T0, T7 and T21. Comparison among (e) T7 and (f) T21 systems.

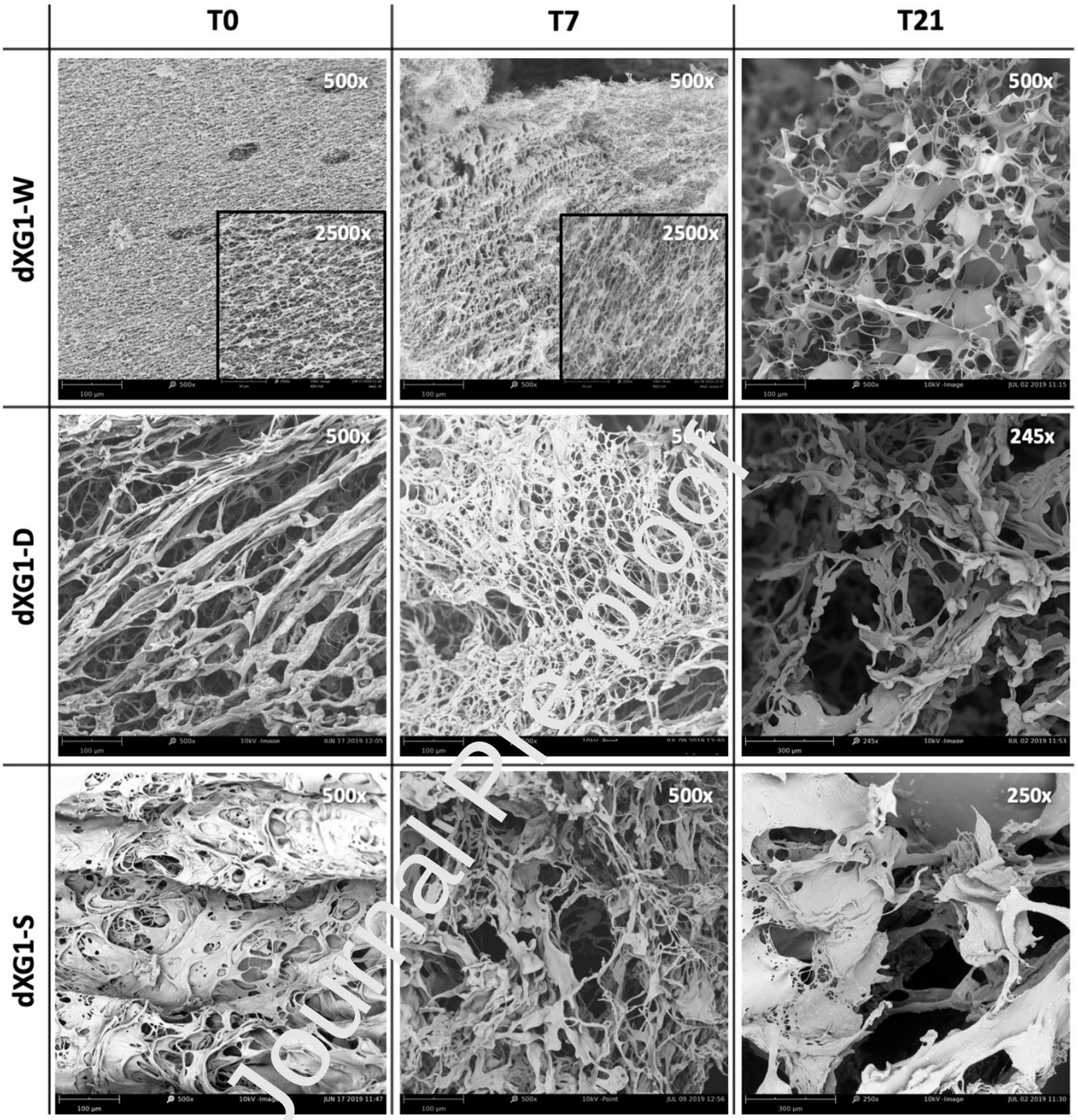

Figure 4. SEM micrographs of "mixed systems" cross-sections at various incubations times.

3.4 Incubation of pre-formed gels with different media

As discussed above, the dXG2UP condition was studied to investigate stem cell viability in case of separate injections of scaffold precursors and stem cells. The mechanical spectra of the dXG2UP-W, dXG2UP-D and dXG2UP-S systems at day 7 and day 21 of incubation are shown in Figure 5a, Figure 5b, and Figure 5c, respectively. The curves relative to dXG2 T0 are also reported for comparison. dXG2UP-W shows a progressive slight increase of storage modulus, and loss modulus with time. The curves also become more frequency-dependent, suggesting that the prolonged incubation is contributing to create a more heterogenous network in terms of crosslink lifetimes. For dXG2UP-D, both storage and loss moduli increase and become more

frequency-dependent after 7 days and slightly decrease at T21. dXG2UP-S T7 shows a marked increase of both storage and loss moduli after the first 7 days and a significant decrease at T21.

The comparison between the three systems at the same incubation time is shown in Figures 5d and 5e, for T7 and T21, respectively. At T7, the adsorption of the two more complex media, DMEM and SCM, by the dXG2 hydrogel has contributed to increase the hydrogel stiffness with respect to the control system (dXG2UP-W). At T21, no significant differences among the systems can be appreciated, similarly to the T7 condition for the mixed systems.

In Figure 6, the morphology of dXG2UP-W T7 and T21 hydrogels is shown. The incubation for 7 days evidences the fairly regular, layered morphology with orthogonally stacked lamellae interconnected by bridge fibres, organisation that partially survives also after 21 days incubation. It is worth noting that, even after prolonged incubation, the average pores size of dXG2UP-W systems is much smaller than the one of the corresponding dXG1-W systems. Hence, the addition of solvent soon after gelation does not bring the system to the same structural organisation of the system that is directly formed from a more diluted polymer dispersion. This means that the concentration of the dispersion at which the network is formed strongly affects the hydrogel evolution in time. The composition of the medium affects the dXG2UP network in a similar way as for the "mixed systems" even though with an appreciable temporal delay. The dXG2UP-S T21 resembles the dXG1-S T0, while the dXG2UP-D T21 is similar to the dXG1-D T7. The temporal delay in the morphology evolution can be explained on the account of the longer relaxation times and slower segmental dynamics that characterise the hydrogels produced at higher polymer concentration. This further supports our conclusion that these networks form under the kinetic control of a frustrated phase-separation that make these scaffolds evolve in a fairly predictive way.

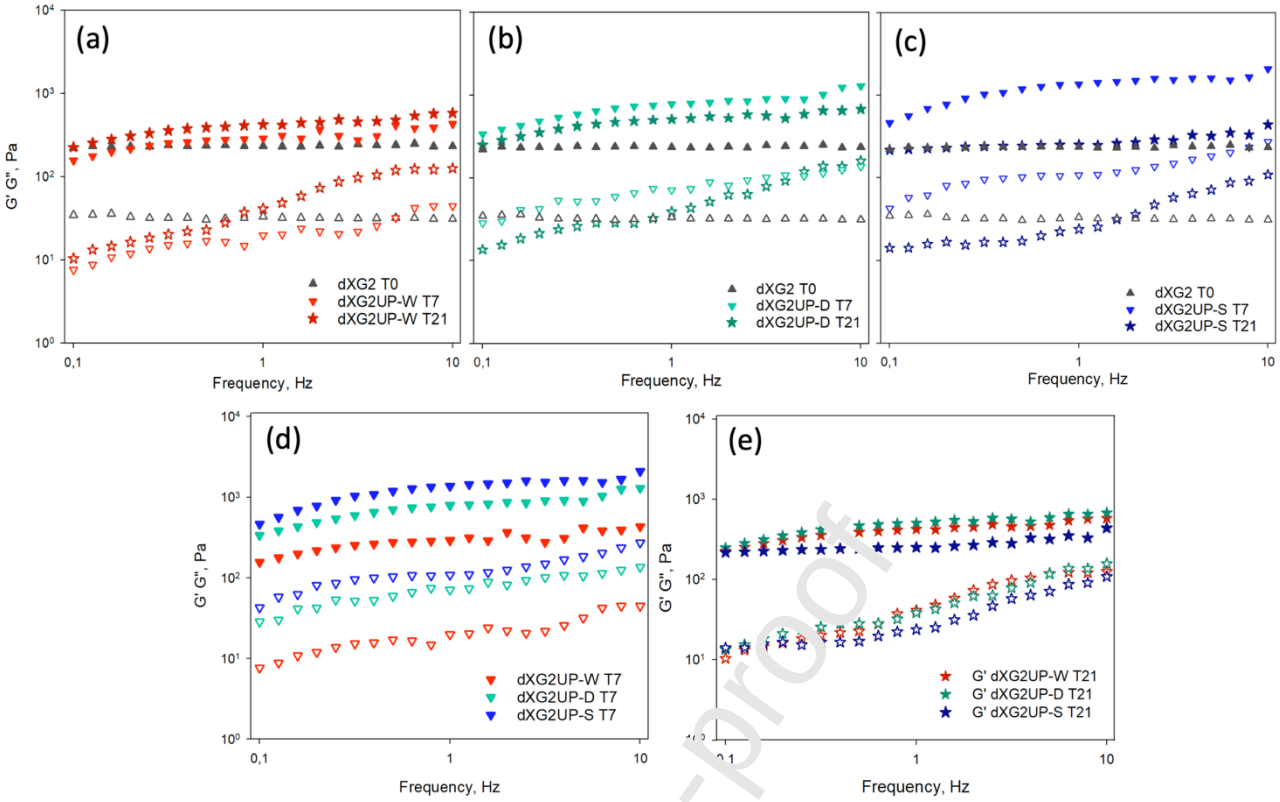

Figure 5. Storage modulus, G' (full dot), and loss modulus, G" (hollow dot), as function of frequency of: (a) dXG2 T0, dXG2UP-W T7 and T21; (b) dXG2 T0, dXG2UP-D T7 and T21; (c) dXG2 T0, dXG2UP-S T7 and T21; comparison among the three (d) T7 and (e) T21 systems.

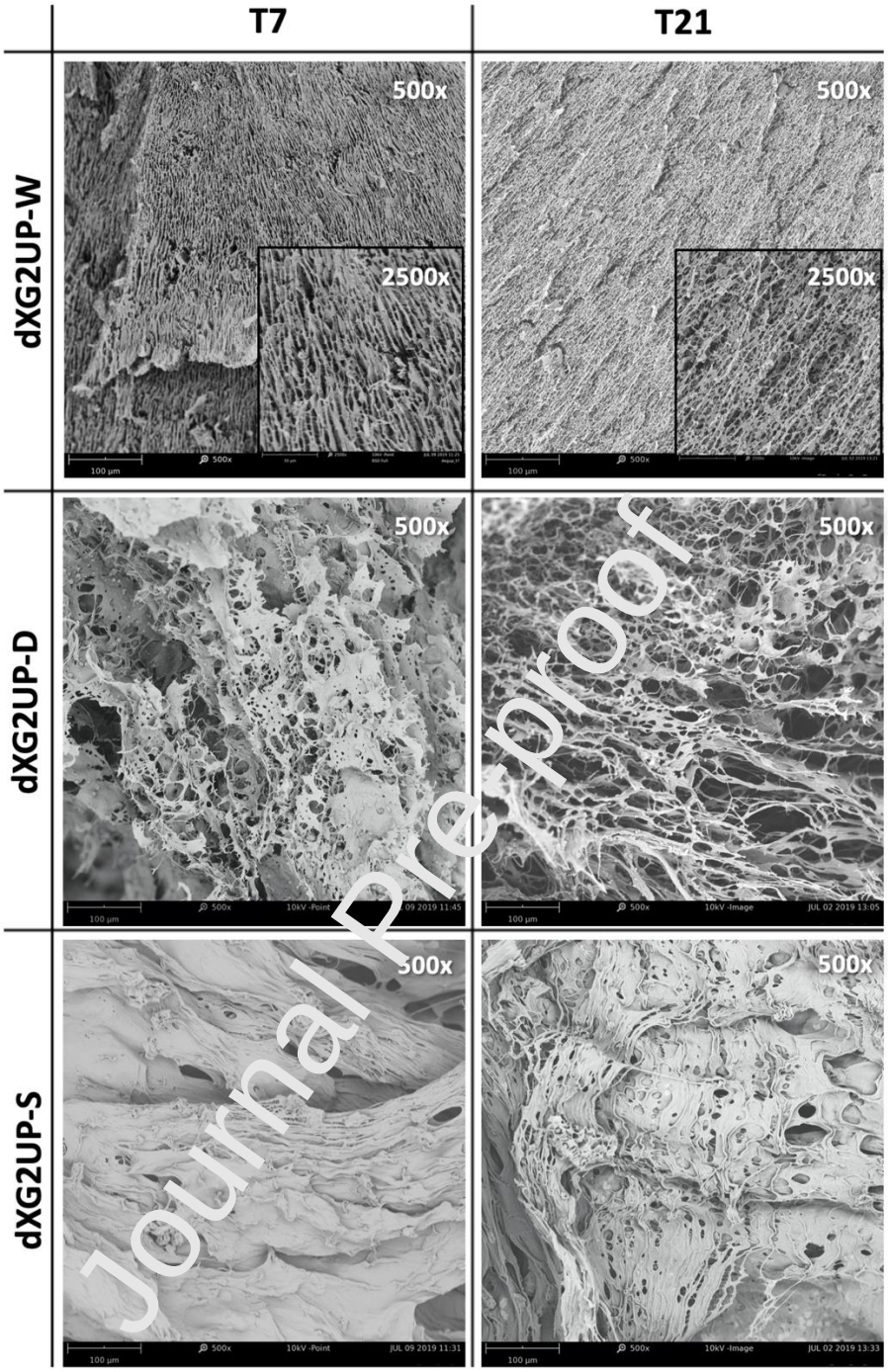

Figure 6. SEM micrographs of cross-sections of freeze-dried samples of dXG2 systems at various incubations times.

3.5 Biological evaluation

In order to verify that the *in-situ* forming dXG hydrogels can be suitable as injectable matrices for stem cell administration and/or confinement into precise anatomic parts of the patient's body, both fluctuating SASCs and adherent ASCs ~~(Figure 7a)~~ were either mixed with dXG2 dispersions or seeded on top of the dXG2 hydrogel and counted. SASCs and ASCs were used after 10 days of *in vitro* 3D and 2D culture, respectively.

Cell morphology both in the "mixed systems" and in the "up systems" was inspected under the light microscope after 1 day (T1), 7 days (T7) and 21 days (T21), to assess eventual

alterations and evident signs of apoptosis (Figure 7a-b). In particular, SASCs show their pristine morphology in both mixed and up conditions up to 21 days. They also seem to integrate well with the hydrogel. On the contrary, ASCs show signs of suffering in both culture conditions already after at 7 days, as indicated by the presence of suspended cell assemblies. This phenomenon is particularly evident for the dXG2UP system.

A quantitative analysis of cell viability was performed by MTS analysis (Figure 8a). Test results confirm the maintenance of viability of SASCs up to 21 days, both in mixed and up conditions ($P<0.001$ versus the counterpart ASCs-2D systems), and the decrease of cell viability for the 2D-cultured cells, that is of about 50% for the mixed condition and 80% for the up condition, after 7 days. In the following two weeks, the ASCs incorporated inside the hydrogel partially recover their viability, reaching an average value of 63%, while the ASCs that were seeded on top do not. Therefore, even if the survival rate of ASCs after 7 days is fairly low, when they were embedded in the dXG1-D matrix, the residual population of alive cells seems able to expand.

To further support the MTS test results of the mixed systems with either SASCs or ASCs, the apoptotic and necrotic profiles of cells recovered from the hydrogels after 21 days culture were evaluated by Annexin V-PI counterstaining. In particular, most of the SASC population resulted Hoechst-positive, hence viable, with only 3% double positive cells to Annexin V and PI (in late stage of apoptosis). On the contrary, for the ASC population, 20% of cells are double positive and 40% are PI-positive only, necrotic cells (Figure 8b-c). The percentage (about 40%) of non-viable cells, counted using the MTS test, is in good agreement with the number of dead cells for late apoptotic and necrotic events, as determined by cell death assay. The combined approach of measuring metabolic activity and assessing membrane integrity suggests significant differences in terms of viability and cell death between the SASCs and ASCs cultured in the same microenvironment.

To evaluate the maintenance of SASCs stemness when the cells mixed with dXG1, a gene and protein expression analysis of pluripotency related markers was performed on both the recovered cells and control system after 21 days of culture. The Realtime PCR analysis reveal a 7-fold increase of the expression of SOX2 ($P< 0.001$) and about 2-fold increase in NANOG with respect to SASCs. The levels of mRNA POU5F1 are similar for the two conditions (Figure 9a). Immunofluorescence analysis was carried out to evidence the nuclear expression of SOX2. The z-stack visualization of confocal microscopy images, shown in Figure 9b, confirms the presence of SOX2 positive cells in SASCs-3D dXG1-S.

We can conclude that adherent ASCs seem not to find optimal conditions for their survival when transferred from the 2D plate to the hydrogels, although when they were incorporated inside the matrix after 7 days they recover some proliferation ability. Conversely, SASCs remain always viable and maintain their stemness when they are incorporated in the 3D matrix. The most interesting finding was a significant increase of SOX2 expression levels in the SASCs-3D mixed with dXG1-S, that is one of the main transcriptional factors for the maintenance of the pluripotency and self-renewal ability in mesenchymal stem cells [55]. SASCs are also viable when cultivated on top of the hydrogel slab. We can speculate that this is because they have not developed a specific pattern of membrane adhesion proteins yet, as they do have when previously cultured on plastic plates (ASCs) [56-58]. This aspect will be further investigated in the development of this research.

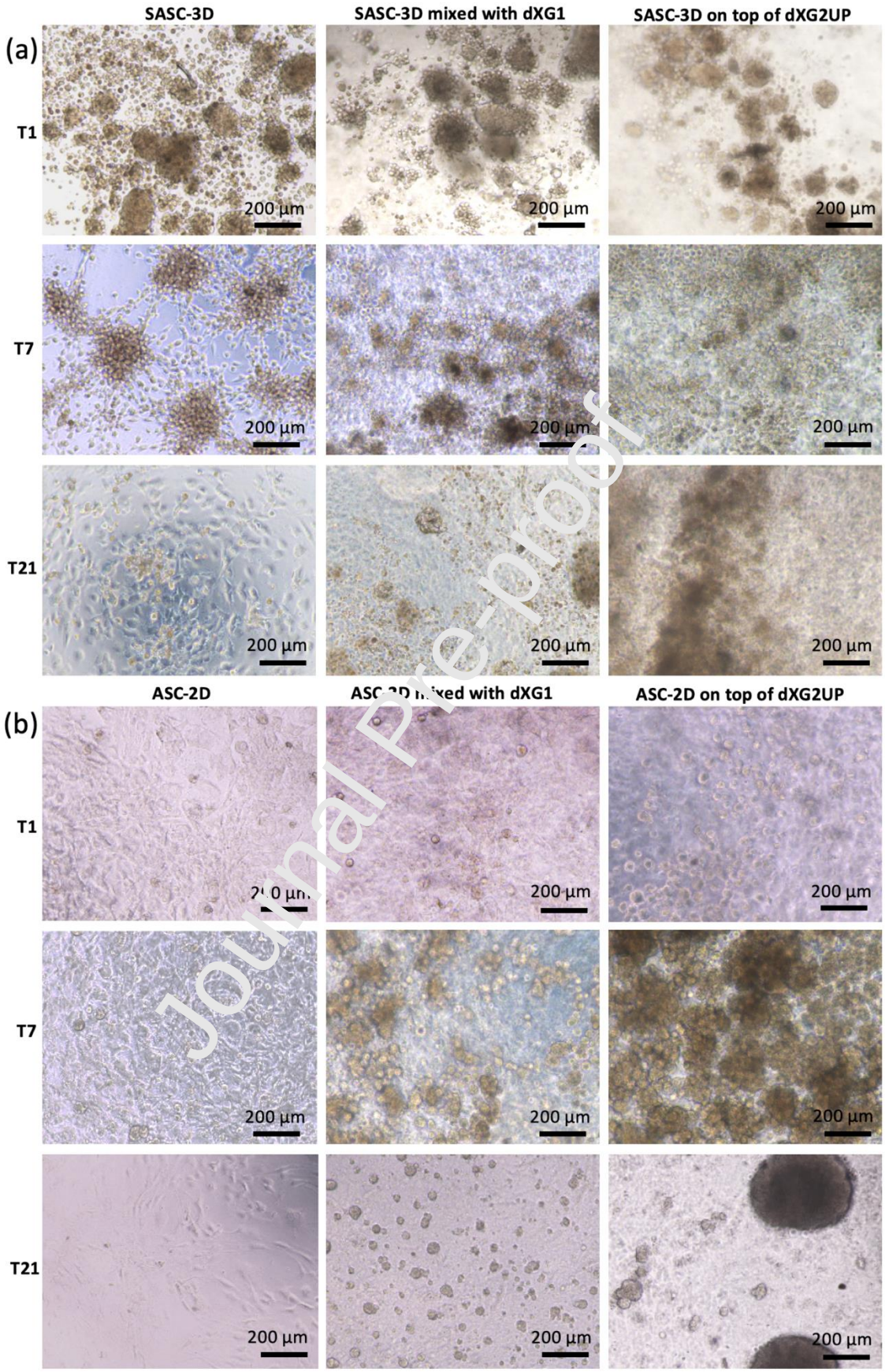

Figure 7. Light microscopy images of (a) SASCs mixed with dXG1-S and seeded on top of dXG2UP-S hydrogels; (b) ASCs mixed with dXG1-D and seeded on top of dXG2UP-D hydrogels, at day 1 (T1), days 7 (T7) and 21 (T21) of *in vitro* culture.

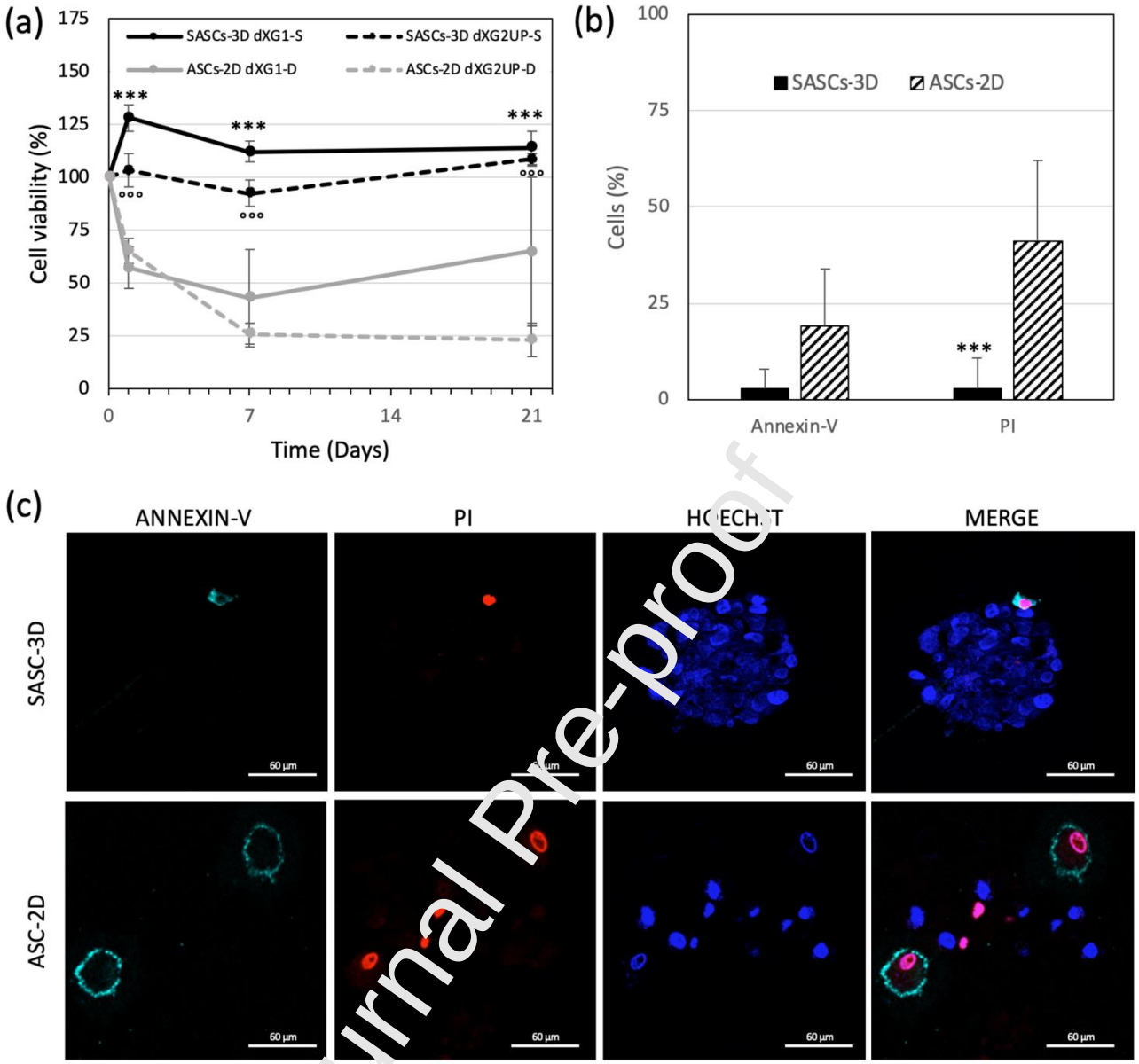

Figure 8. (a) Cell viability by MTS at 1 day, 7 days and 21 days of *in vitro* culture. (b) Percentage of positive cells to Annexin-V/Propidium iodide staining. (c) Representative images of Annexin V (cyan), PI (red), Hoechst (blue) and merge positive cells of recovered SASCs-3D and ASCs-2D to dXG1 after 21 days of *in vitro* culture.

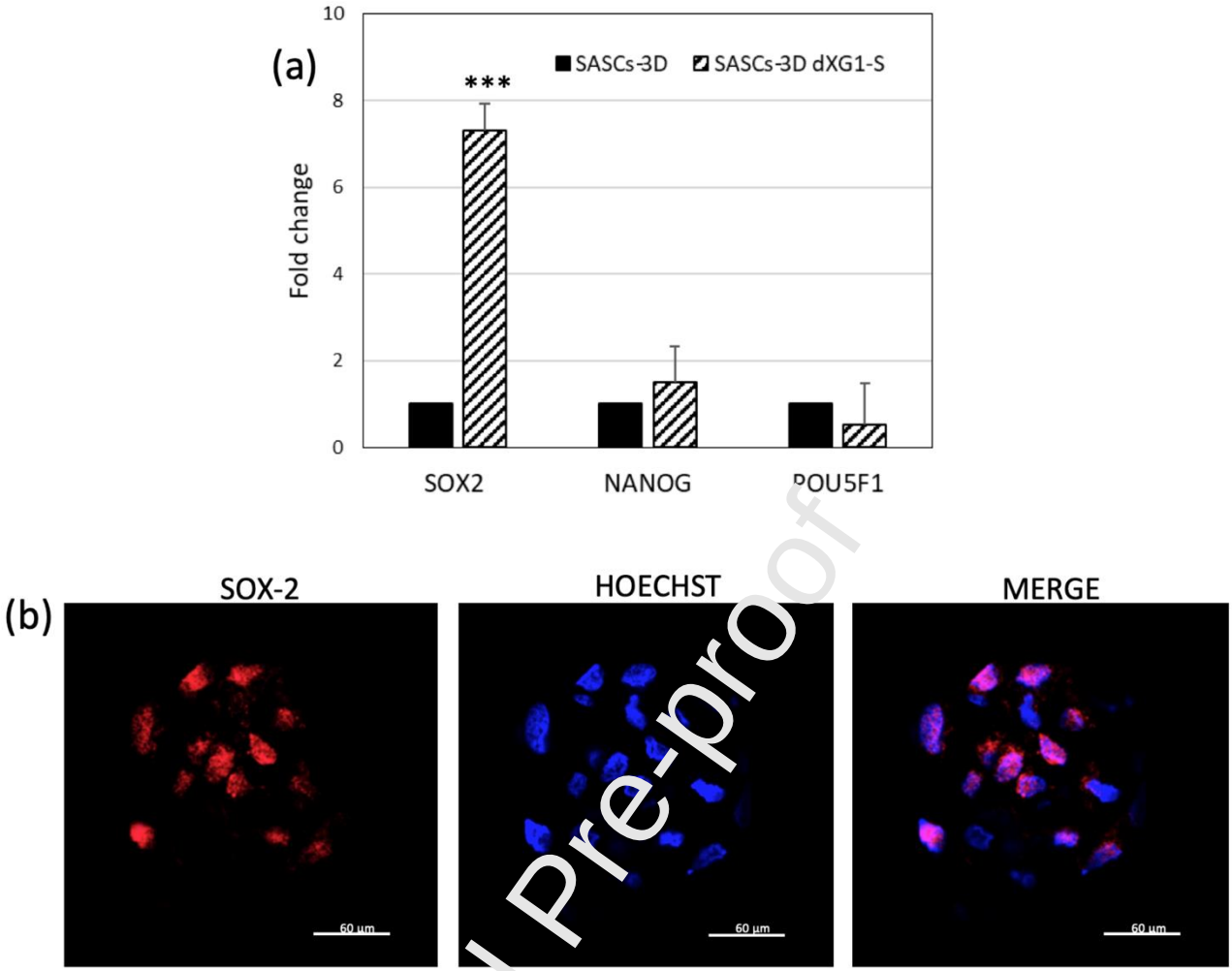

Figure 9. (a) Relative gene expression fold change of SOX2, NANOG and POU5F1 in SASCs-3D (control) and recovered cells from SASCs-3D dXG1-S; (b) nuclear SOX2 (red), Hoechst (blue) and merge positive cells in SASCs-3D dXG1-S. Analyses performed after 21 days of *in vitro* culture.

3.6 Injectability of dXG1-S dispersion mixed with SASCs

In order to evaluate the suitability of the dXG1-S dispersion mixed with SASCs to be directly administered in the site of the lesion, the shear viscosity of the system loaded with SASCs was measured and compared to the analogous system without cells. Moreover, the dynamic-mechanical behavior in small amplitude oscillation conditions of the hydrogel formed from dXG1-S mixed with SASCs and injected directly on the rheometer plate with a syringe equipped with G23 needle was investigated, to assess the effect of both cells and injection on the mechanical properties of the hydrogel. Finally, cell viability of SASCs injected together with the dXG1-S dispersion was ascertained.

The dXG1-S dispersion is liquid-like at 4°C and quickly gel when heated at 37°C. The apparent viscosity as function of shear rate of the dXG1-S dispersion with and without cells was measured at 25°C. The flow curves, shown in Figure 10a, are typical of pseudo-plastic fluids. The viscosity decreases with the increase of the shear rate, leading to a shear thinning region, as a result of the decrease in number of chain entanglements when chains orient themselves according to the flow direction. The presence of SASCs in the formulation leads to lower viscosities at low shear rates likely because the spheroids reduce the number of chain

entanglements. Being the apparent viscosity almost always below 0.1 Pa s, according to the viscosity-needle ID-glide force correlations shown by Watt et al. 2019 [59] the expected glide force with a G23 syringe needle is lower than 5 N, that is well below the highest recommended glide force value of 20 N (ISO guidance 11,608-3, sez. 4.3).

Dynamic mechanical rheological analysis as function of frequency was performed injecting the dXG1-S dispersion with and without SASCs directly onto the rheometer lower plate and letting it equilibrate to 37°C for 10 minutes. The mechanical spectra show that the injection does not affect G' and G" moduli of both cell-laden and cell-devoid hydrogels. Indeed, G' and G" curves overlap with those of the systems with the same composition but not extruded through the syringe needle. On the other hand, the presence of SASCs causes an increase of G' curve only. We can conclude that the spheroids do not obstacle the network formation, but actually act as filler reinforcement, filling its large pores. Furthermore, SASCs embedded in dXG1-S maintained their viability also after passage through G23 syringe needles (Figure 10c), supporting their potential uses for tissue repair processes with minimally invasive procedures.

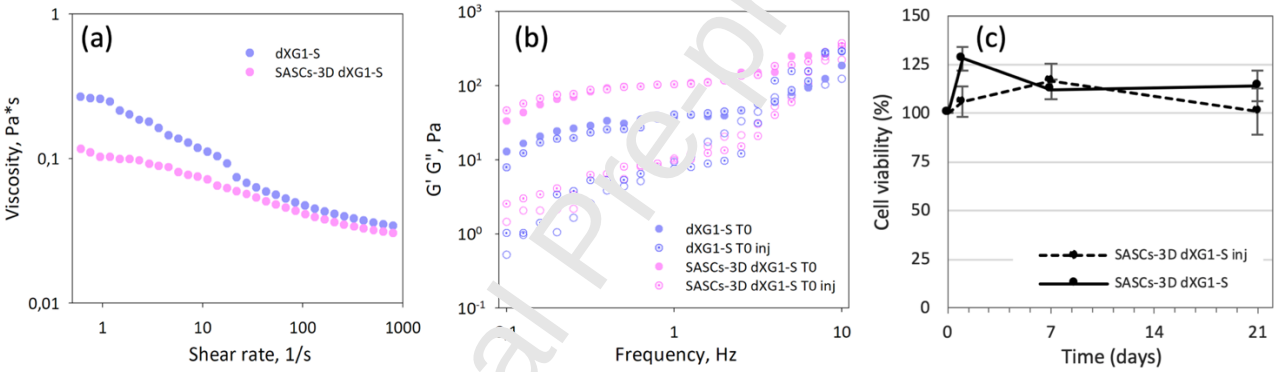

Figure 10. (a) Shear viscosity of dXG1-S and SASC-3D dXG1-S as function of shear rate; (b) storage modulus, G' (full dot), and loss modulus, G" (hollow dot), of dXG1-S T0 and SASC-3D dXG1-S T0 before and after injection (inj) as function of frequency; (c) cell viability by MTS of SASC-3D dXG1-S T0 before and after injection (inj) at 1 day, 7 days and 21 days of in vitro culture.

Conclusions

Spheroids of human adipose tissue-derived stem cells have a number of advantages over 2D cultured stem cells that make them a very attractive autologous cell source for aesthetic and reconstructive surgery. In order to fully exploit the regenerative potential of these cells, effective strategies for their administration in confined anatomic areas of the body and creation of microenvironments that also ensure optimal cell viability are required. Partially degalactosylated xyloglucan, with ca. 45% degalactosylation degree, is a biocompatible polymer that when dispersed into aqueous media rapidly set into durable hydrogels at body temperature. The physical networks form under kinetic control of a phase-separation process that is frustrated by the sudden increase of system viscosity and affected by both polymer concentration and composition of the aqueous phase. In particular, the high saline content of DMEM leads to the development of a fibrous network, whereas SCM favors fusion of dXG chains into extended hollow thin membranes. Upon incubation at body temperature cooperative chain segment dynamics are activated and modify the network structure, stiffness

and porosity. In general, dXG1 systems show random and heterogeneous porosity that increases in size with incubation time, due to slow erosion. dXG2 presents a more compact structure with a multi-layered morphology. The temporal delay in the morphology evolution at the increase of polymer concentration can be explained on the account of the longer relaxation times and slower segmental dynamics that characterise the hydrogels. Culturing SASCs within or on top of dXG hydrogels preserve cells vitality and stemness up to three weeks.

These results encourage to continue on the exploration of biological behavior of SASCs in dXG matrices in terms of differentiation abilities in different cell lineages, both in the presence and in the absence of purposely added specific signaling factors to fully exploit their potential in minimally invasive and personalized regenerative medicine interventions. Moreover, the influence of stem cell secreted factors on the hydrogel properties remains to be investigated.

Conflicts of interest

There are no conflicts to declare.

Acknowledgements

Authors wish to thank Dr. Alice Conigliaro of the University of Palermo for her support with confocal analysis and ATeN Center of University of Palermo, "Proteomica e Genomica" and "Preparazione e Analisi dei Biomateriali" laboratories, for technical support. Clelia Dispenza acknowledges the FFR_D09-Fondo di Finanziamento per la Ricerca di Ateneo 2018/2021.

Bibliography

[1] I.U. Schraufstatter, R.G. Discipio, S. Khaldoyanidi, Mesenchymal stem cells and their microenvironment, Front Biosci (Landmark Ed). 16 2271-88. 2011.

[2] J.M. Gimble, A.J. Katz, B.A. Bunnell, Adipose-derived stem cells for regenerative medicine, Circ. Res.100 (2007) 1249-60. doi.org/10.1007/s11010-017-3265-9.

[3] M. Oberringer, M. Bubel, M. Jennewein, S. Guthörl, T. Morsch, S. Bachmann, W. Metzger, T. Pohlemann, The role of adipose-derived stem cells in a self-organizing 3D model with regard to human soft tissue healing, Mol. Cell. Biochem. 445 (2018) 195-210. doi.org/10.1007/s11010-017-3265-9.

[4] Y. Kim, P. Baipaywad, Y. Jeong, H. Park, Incorporation of gelatin microparticles on the formation of adipose-derived stem cell spheroids, Int. J. Biol. Macromol. 110 (2018) 472-8. doi:10.1016/j.ijbiomac.2018.01.046.

[5] A.B. Di Stefano, A.A. Leto Barone, A. Giammona, T. Apuzzo, P. Moschella, S. Di Franco, G. Giunta, M. Carmisciano, C. Eleuteri, M. Todaro, F. Dieli, A. Cordova, G. Stassi, F. Moschella, Identification and Expansion of Adipose Stem Cells with Enhanced Bone Regeneration Properties, J. Regen. Med. 5 (2015) 1-11. doi.org/10.4172/2325-9620.1000124.

[6] A.B. Di Stefano, L. Montesano, B. Belmonte, A. Gulino, C. Gagliardo, A.M. Florena, G. Bilello, F. Moschella, A. Cordova, A.A. Leto Barone, F.Toia, Human spheroids from adipose-derived stem cells induce calvarial bone production in AQ1 a xenogeneic rabbit model, Ann. Plast. Surg. 2020. In press.

[7] A.B. Di Stefano, F. Grisafi, M. Castiglia, A. Perez, L. Montesano, A. Gulino, F. Toia, D. Fanale, A. Russo, F. Moschella, A.A. Leto Barone, A. Cordova, Spheroids from adipose-derived stem cells exhibit an miRNA profile of highly undifferentiated cells, J. Cell. Physiol. 233 (2018) 8778-89. doi:10.1002/jcp.26785.

[8] G. Shim, S. Lee, J. Han, G. Kim, H. Jin, W. Miao, T.-G. Yi, Y.K. Cho, S.U. Song, Y.-K. Oh, Pharmacokinetics and in vivo fate of intra-articularly transplanted human bone marrow-derived clonal mesenchymal stem cells, Stem Cells Dev. 24 (2015) 1124-32. doi:10.1089/scd.2014.0240.

[9] J.S. Hyun, M.C. Tran, V.W. Wong, M.T. Chung, D.D. Lo, D.T. Montoro, D.C. Wan, M.T. Longaker, Enhancing stem cell survival in vivo for tissue repair, Biotechnol, Adv. 31 (2013) 736-43. doi:10.1016/j.biotechadv.2012.11.003.
[10] C. Kan, L. Chen, Y. Hu, H. Lu, Y. Li, J.A. Kessler, L. Kan, Microenvironmental factors that regulate mesenchymal stem cells: lessons learned from the study of heterotopic ossification, Histol. Histopathol. 32 (2017) 977-85. doi:10.14670/HH-11-890.
[11] S. Agarwal, S. Loder, D Cholok, J. Li, C. Breuler, J. Drake, C. Brownley, J. Peterson, S. Li, B. Levi, Surgical Excision of Heterotopic Ossification Leads to Re-Emergence of Mesenchymal Stem Cell Populations Responsible for Recurrence, Stem Cells Transl. Med. 6 (2017) 799-806. doi:10.5966/sctm.2015-0365.
[12] Q.L. Loh, C. Choong, Three-dimensional scaffolds for tissue engineering applications: role of porosity and pore size, Tissue Eng. Part B Rev. 19 (2013) 485-502. doi:10.1089/ten.TEB.2012.0437.
[13] Y. Zhou, H. Chen, H. Li, Y. Wu, 3D culture increases pluripotent gene expression in mesenchymal stem cells through relaxation of cytoskeleton tension, J. Cell. Mol. Med. 21 (2017) 1073-84. doi:10.1111/jcmm.12946.
[14] X. Meng, P. Leslie, Y. Zhang, J. Dong, Stem cells in a three-dimensional scaffold environment, Springerplus. 3 (2014) 80. doi:10.1186/2193-1801-3-80.
[15] J. Zhu, R.E. Marchant, Design properties of hydrogel tissue-engineering scaffolds, Expert Rev. Med. Devices 8 (2011) 607-26. doi:10.1586/erd.11.27.
[16] S. Allazetta, T.C. Hausherr, M.P. Lutolf, Microfluidic synthesis of cell-type-specific artificial extracellular matrix hydrogels, Biomacromolecules (2013) 14 1122-31. doi.org/10.1021/bm4000162.
[17] L. Nayyer, K.H. Patel, A. Esmaeili, R.A. Rippel, M. Birchall, G. O'toole, et al. Tissue engineering: revolution and challenge in auricular cartilage reconstruction, Plast. Reconstr. Surg. 129 (2012) 1123-37. doi:10.1097/PRS.0b013e31824a2c1c.
[18] M.J. Stoddart, S. Grad, D. Eglin, M. Alini, Cells and biomaterials in cartilage tissue engineering, Regen. Med. 4 (2009) 81-98. doi.org/10.2217/17460751.4.1.81.
[19] T. Hoshiba, H. Lu, N. Kawazoe, G. Chen, Decellularized matrices for tissue engineering, Expert Opin. Biol. Ther. 10 (2010) 1717-28. doi:10.1517/14712598.2010.534079.
[20] L.E. Fitzpatrick, T.C. McDevitt, Cell-derived matrices for tissue engineering and regenerative medicine applications. Biomater. Sci. 2015;3:12-24. doi:10.1039/C4BM00246F.
[21] S. Rao Pattabhi, J.S. Martinez, T.C. Keller, Decellularized ECM effects on human mesenchymal stem cell stemness and differentiation, Differentiation. 88 (2014) 131-43. doi:10.1016/j.diff.2014.12.005.
[22] N.A. Dzhoyashvili, S. Shen, Y.A. Rochev, Natural and Synthetic Materials for Self-Renewal, Long-Term Maintenance, and Differentiation of Induced Pluripotent Stem Cells, Adv. Healthc. Mater. 4 (2015) 2342-59. doi:10.1002/adhm.201400798.
[23] B.K. Velmurugan, L. Bharathi Priya, P. Poornima, L.J. Lee, R. Baskaran, Biomaterial aided differentiation and maturation of induced pluripotent stem cells, J. Cell. Physiol. 234 (2019) 8443-54. doi:10.1002/jcp.27769.
[24] H. Geckil, F. Xu, X. Zhang, S. Moon, U. Demirci, Engineering hydrogels as extracellular matrix mimics, Nanomedicine (Lond) 5 (2010) 469-84. doi:10.2217/nnm.10.12.
[25] B.A. Aguado, W. Mulyasasmita, J. Su, K.J. Lampe, S.C. Heilshorn, Improving viability of stem cells during syringe needle flow through the design of hydrogel cell carriers, Tissue Eng. Part A 18 (2012) 806-15. doi:10.1089/ten.TEA.2011.0391.
[26] Y. Liang, P. Walczak, J.W. Bulte The survival of engrafted neural stem cells within hyaluronic acid hydrogels. Biomaterials 34 (2013) 5521-9. doi:10.1016/j.biomaterials.2013.03.095.
[27] K.H. Hong, Y.M. Kim, S.C. Song, Fine-Tunable and Injectable 3D Hydrogel for On-Demand Stem Cell Niche, Adv. Sci. (Weinh) 6 (2019) 1900597. doi.org/10.1002/advs.201900597.

[28] D. Chen, P. Guo, S. Chen, Y. Cao, W. Ji, X. Lei, L. Liu, P. Zhao, R. Wang, C. Qi, Y. Liu, H. He, Properties of xyloglucan hydrogel as the biomedical sustained-release carriers, J. Mater. Sci. Mater. Med. 23 (2012) 955-62. doi.org/10.1007/s10856-012-4564-z.
[29] S. Miyazaki, N. Kawasaki, W. Kubo, K. Endo, D. Attwood, Comparison of in situ gelling formulations for the oral delivery of cimetidine, Int. J. Pharm. 220 (2001) 161-8. doi.org/10.1016/S0378-5173(01)00669-X.
[30] I.C.M. Dea, Industrial Polysaccharides, Pure Appl. Chem. 61, 7 (1989) 1315-22.
[31] S.C. Fry, The structure and functions of xyloglucan, J. Exp. Bot. 40 (1989) 1-12. doi.org/10.1093/jxb/40.1.1.
[32] S. Yamanaka, Y. Yuguchi, H. Urakawa, K. Kajiwara, M. Shirakawa, K. Yamatoya, Gelation of tamarind seed polysaccharide xyloglucan in the presence of ethanol, Food Hydrocoll. 14 (2000) 125-8. doi.org/10.1016/S0268-005X(99)00057-0.
[33] M. Shirakawa, K. Yamatoya, K. Nishinari, Tailoring of xyloglucan properties using an enzyme, Food Hydrocoll. 12 (1998) 25-8. doi.org/10.1016/S0268-005X(98)00052-6.
[34] Y. Chandramouli, S. Firoz, A. Vikram, B. Mahitha, Y.E. Rubia, K. Hemanthpavankumar, Tamarind seed polysaccharide (TSP) - an adaptable excipient for novel drug delivery systems, Intern. J. Pharm. Pract. Drug Res. (2012) 57-63.
[35] S. Miyazaki, F. Suisha, N. Kawasaki, M. Shirakawa, K. Yamatoya, D. Attwood, Thermally reversible xyloglucan gels as vehicles for rectal drug delivery, J. Control. Release 56 (1998) 75-83. doi.org/10.1016/S0168-3659(98)00079-0.
[36] N. Kawasaki, R. Ohkura, S. Miyazaki, Y. Uno, S. Sugimoto, D. Attwood, Thermally reversible xyloglucan gels as vehicles for oral drug delivery, Int. J. Pharm. 18(1999) 227-34. doi.org/10.1016/S0378-5173(99)00026-5.
[37] A. Takahashi, S. Suzuki, N. Kawasaki, W. Kubo, S. Miyazaki, R. Loebenberg, J. Bachynsky, D. Attwood, Percutaneous absorption of non-steroidal anti-inflammatory drugs from in situ gelling xyloglucan formulations in rats, Int. J. Pharm. 246 (2002) 179-86. doi:10.1016/s0378-5173(02)00394-0.
[38] A.D. Kulkarni, A.A. Joshi, C.L. Patil, P.D. Amale, H.M. Patel, S.J. Surana, V. S. Belgamwar, K.S. Chaudhari, C.V. Pardeshi, Xyloglucan: A functional biomacromolecule for drug delivery applications, Int. J. Biol. Macromol. 104 (2017) 799-812. doi.org/10.1016/j.ijbiomac.2017.06.088.
[39] D.R. Nisbet, K.E. Crompton, S.D. Hamilton, S. Shirakawa, R.J. Prankerd, D.I. Finkelstein, M.K. Horne, J.S. Forsythe, Morphology and gelation of thermosensitive xyloglucan hydrogels, Biophys Chem. 121 (2006) 14-20. doi.org/10.1016/j.bpc.2005.12.005.
[40] D.R. Nisbet, D. Moses, T.R. Gengenbach, J.S. Forsythe, D.I. Finkelstein, M.K. Horne, Enhancing neurite outgrowth from primary neurones and neural stem cells using thermoresponsive hydrogel scaffolds for the repair of spinal cord injury, J. Biomed. Mater. Res. A. 89(2009) 24-35. doi:10.1002/jbm.a.31962.
[41] C. Dispenza, S. Todaro, D. Bulone, M.A. Sabatino, G. Ghersi, P.L. San Biagio, C. Lo Presti, Physico-chemical and mechanical characterization of in-situ forming xyloglucan gels incorporating a growth factor to promote cartilage reconstruction, Mater. Sci. Eng. C Mater. Biol. Appl. 70 (2017) 745-52. doi:10.1016/j.msec.2016.09.045.
[42] M.M.T. do Rosário, G.R. Noleto, C.L. de Oliveira Petkowicz, Degalactosylation of xyloglucans modify their pro-inflammatory properties on murine peritoneal macrophages, Int. J. Biol. Macromol. 105 (2017) 533-40. doi.org/10.1016/j.ijbiomac.2017.07.068.
[43] M. Todaro, M.P. Alea, A.B. Di Stefano, P. Cammareri, L. Vermeulen, F, Iovino C. Tripodo, A. Russo, G. Gulotta, J.P. Medema, G. Stassi, Colon cancer stem cells dictate tumor growth and resist cell death by production of interleukin-4, Cell Stem. Cell. 1 (2007) 389-402. doi:10.1016/j.stem.2007.08.001.
[44] A.K.A.S. Brun-Graeppi, C. Richard, M. Bessodes, D. Scherman, T. Narita, G. Ducouret, O. Merten, Study on the sol–gel transition of xyloglucan hydrogels, Carbohydr. Polym. 80(2) (2010) 555-62. doi.org/10.1016/j.carbpol.2009.12.026.

[45] P. Lang, W. Burchard, Structure and aggregation behavior of tamarind seed polysaccharide in aqueous solution, Macromol. Chem. Phys. 194(11) (1993) 3157-66. doi.org/10.1002/macp.1993.021941119.
[46] S. Todaro, C. Dispenza, M.A. Sabatino, M.G. Ortore, R. Passantino, P.L. San Biagio, D. Bulone, Temperature-induced self-assembly of degalactosylated xyloglucan at low concentration, J. Polym. Sci. Part B: Polym. Phys. 53 (2015) 1727–35. doi.org/10.1002/polb.23895.
[47] K.J. Livak, T.D. Schmittgen, Analysis of relative gene expression data using real-time quantitative PCR and the 2(-Delta Delta C(T)) Method, Methods 25(4) (2001) 402-8. doi:10.1006/meth.2001.1262.
[48] M. Grassi, R. Lapasin, S. Pricl, A srudy of the rheological behavior of scleroglucan weak gel systems, Carbohydr. Polym. 29 (2) (1996) 169-81. doi.org/10.1016/0144-8617(95)00120-4.
[49] M. Han, Y. Liu, F. Zhang, D. Sun, J. Jiang, Effect of galactose side-chain on the self-assembly of xyloglucan macromolecule, Carbohydr. Polym. 246 (2020) 116577. doi.org/10.1016/j.carbpol.2020.116577.
[50] C. Dispenza, S. Todaro, M.A. Sabatino, D. Chillura Martino, V.Martorana, P.L.San Biagio, P. Maffei, D. Bulone, Multi-scale structural analysis of xyloglucan, Cellulose 27 (2020) 3025-35. doi.org/10.1007/s10570-020-03004-0.
[51] Y. Xu, C. Wang, K.C. Tam, L. Li, Salt-assisted and salt-suppressed sol-gel transitions of methylcellulose in water, Langmuir 20 (2004) 646-52. doi.org/10.1021/la0356295.
[52] D. Giacomazza, D. Bulone, P.L. San Biagio, R. Marino, R. Lapasin, The role of sucrose concentration in self-assembly kinetics of high methoxyl pectin, Int. J. Biol. Macromol. 112 (2018) 1183-90. doi.org/10.1016/j.ijbiomac.2018.02.103.
[53] L.A. Ditta, D. Bulone, P.L. San Biagio, R. Marino, D. Giacomazza, R. Lapasin, The degree of compactness of the incipient High Methoxyl Pectin networks. A rheological insight at the sol-gel transition, Int. J. Biol. Macromol. 158 (2020) 985-93. doi.org/10.1016/j.ijbiomac.2020.05.019.
[54] C.N. Sakakibara, M.R. Sierakowski, R.R. Ramírez, C. Chassenieux, I. Riegel-Vidotti, R.A. de Freitas, Salt-induced thermal gelation of xyloglucan in aqueous media, Carbohydr. Polym. 223 (2019) 115083. doi.org/10.1016/j.carbpol.2019.115083.
[55] D.S. Yoon, Y. Choi, Y. Jang, M. Lee, W.J. Choi, S.H. Kim, J.W: Lee, SIRT1 directly regulates SOX2 to maintain self-renewal and multipotency in bone marrow-derived mesenchymal stem cells, Stem Cells. 32 (2014) 3219-31. doi.org/10.1002/stem.1811.
[56] W. Mueller-Klieser, Multicellular spheroids. A review on cellular aggregates in cancer research, J. Cancer Res. Clin. Oncol. 113 (1987) 101-22. doi.org/10.1007/BF00391431.
[57] N. Naderi, C. Wilde, T. Haque, W. Francis, A.M. Seifalian, C.A. Thornton, Z. Xia, I.S. Whitaker, Adipogenic differentiation of adipose-derived stem cells in 3-dimensional spheroid cultures (microtissue): implications for the reconstructive surgeon, J. Plast. Reconstr. Aesthet. Surg. 67 (2014) 1726-34. doi:10.1016/j.bjps.2014.08.013.
[58] R. Iwai, Y. Nemoto, Y. Nakayama, Preparation and characterization of directed, one-day-self-assembled millimeter-size spheroids of adipose-derived mesenchymal stem cells, J. Biomed. Mater. Res. Part A. 104 (2016) 305-12. doi.org/10.1002/jbm.a.35568.
[59] R.P. Watt, H. Khatri, A.R.G. Dibble, Injectability as a function of viscosity and dosing materials for subcutaneous administration, Int. J. Pharm. 554 (2019) 376-86. doi:10.1016/j.ijpharm.2018.11.012.

CRediT Author Statement

F. Toia: Investigation, Writing-original draft; **A.B. Di Stefano**: Investigation, Writing -original draft, Visualisation; **E. Muscolino**: Investigation, Writing-original draft, Visualisation; **M.A. Sabatino**: Metodology, Supervision; **D. Giacomazza:** Metodology, Supervision; **F. Moschella:** Conceptualisation, Funding acquisition; **A. Cordova:** Conceptualisation, Resources; **C. Dispenza:** Conceptualisation, Resources, Funding acquisition, Writing-Review and Editing. All Authors have reviewed and approved the final manuscript.